ADVANCED FUNCTIONAL MATERIALS
www.afm-journal.de

Tenogenic Induction of Human MSCs by Anisotropically Aligned Collagen Biotextiles

*Mousa Younesi, Anowarul Islam, Vipuil Kishore, James M. Anderson, and Ozan Akkus**

A novel biofabrication modality, electrophoretic compaction with macromolecular alignment, is utilized to make collagen threads that mimic the native tendon's structure and mechanical properties. A device with kinematic electrodes is designed to fabricate collagen threads in continuous length. For the first time, a 3D-biotextile is woven purely from collagen. Mechanical properties and load-displacement behavior of the biotextile mimic those of the native tendon while presenting a porosity of 80%. The open pore network facilitates cell seeding across the continuum of the bioscaffold. Mesenchymal stem cells (MSCs) seeded in the woven scaffold undergo tenogenic differentiation in the absence of growth factors and synthesize a matrix that is positive for tenomodulin, COMP and type I collagen. Up-regulation of tenomodulin, a tendon specific marker, is 11.6 ± 3.5 fold, COMP is up-regulated 16.7 ± 5.5 fold, and Col I is up-regulated 6.9 ± 2.7 fold greater on ELAC threads when compared to randomly oriented collagen gels. These results demonstrate that a bioscaffold woven using collagen threads with densely compacted and anisotropically aligned substrate texture stimulates tenogenesis topographically, rendering the electrochemically aligned collagen as a promising candidate for functional repair of tendons and ligaments.

M. Younesi, A. Islam, O. Akkus
Department of Mechanical and Aerospace Engineering
Case Western Reserve University
Cleveland, OH 44106, USA
E-mail: oxa@case.edu
Prof. V. Kishore
Department of Chemical Engineering
Florida Institute of Technology
Melbourne, FL 32901, USA
Prof. J. M. Anderson
Department of Pathology
Case Western Reserve University
Cleveland, OH 44106, USA
Prof. J. M. Anderson
Department of Macromolecular Science
Case Western Reserve University
Cleveland, OH 44106, USA
Prof. O. Akkus
Department of Orthopedics
Case Western Reserve University
Cleveland, OH 44106, USA
Prof. J. M. Anderson, Prof. O. Akkus
Department of Biomedical Engineering
Case Western Reserve University
Cleveland, OH 44106, USA

DOI: 10.1002/adfm.201400828

1. Introduction

Tendon is a dense collagenous tissue which transmits muscle forces to bone. Tendon disorders are among the most commonly encountered musculoskeletal problems which are caused by trauma, injury or age-related degeneration. In the United States alone, an estimated 30 000 to 75 000 rotator cuff tendon repairs are performed each year, and 40% or more of patients older than 60 years are affected by rotator cuff tendon related disorders. Surgical strategies include the augmentation of the repair site mechanically by various graft materials.[1] Autografts are associated with donor site morbidity and have limited availability for sizeable tendons such as the rotator cuff or the Achilles tendon. Tissue rejection, disease transmission risk and limited porosity are drawbacks associated with allografts and xenografts. While synthetic scaffolds have good mechanical properties, they pose limitations such as poor cell adhesion,[2] chronic inflammation[3] and persistence of foreign body giant cells.[4]

Unlike osteogenesis and chondrogenesis, there are no well accepted growth factor formulations that can induce tenogenesis reliably. Studies generally report tenogenic differentiation under the effect of growth factors at the gene expression level,[5,6] with no or little evidence on matrix production. Several studies have reported tenogenesis under topographical cues, particularly the matrices that present aligned fibers.[7–10] Such materials induce the cells to become elongated under contact guidance. These studies too reported evidence for tenogenic differentiation at the expression level only. Therefore, while there are implications that anisotropic matrix alignment is conducive to tenogenesis, there have been no 3D biomimetic environments which induced tenogenesis at the expression and matrix production levels. Therefore, reports of tenoinduction to date are not conclusive.

Type I collagen is ideal as a scaffold biomaterial because it is the major component of tendon's extracellular matrix (ECM). Collagen is biocompatible and it also presents cell adhesion moieties.[11] However, existing collagen-based scaffolds are in gel or sponge forms which possess weak mechanical strength, limiting collagen's applicability for the repair of load-bearing tendon. It has been shown that collagen molecules can be densely packed and aligned under the effect of electrically induced pH gradients.[7,12,13] Electrocompaction and alignment of molecules as such provides collagen threads that mimic the

native tendon in terms of structural and mechanical properties.[12,13] However, mechanically functional 3D scaffold models using electrochemically aligned collagen (ELAC) threads have not been realized to date. The current study produced ELAC threads in continuous length to enable the fabrication of a woven 3D-biotextile scaffold. The resulting woven biotextile mimicked the structural mechanical properties of the native tendon. Mesenchymal stem cells (MSCs) seeded in woven scaffolds expressed and produced tendon-specific markers.

2. Results

Continuous length ELAC threads were fabricated by a kinematically rotating linear electrode pair (**Figure 1**a) (see the Experimental Section) and crosslinked chemically. Single ELAC threads failed abruptly at the end of the linear elastic region while the ELAC yarn showed a prominent post-yield deformability (**Figure 2**a). The ultimate tensile load of ELAC threads did not increase with increasing fiber diameter (Figure 2b). In association, the ultimate tensile strengths of the threads (Figure 2b) decreased with increasing thread diameter. Twisting three threads as a 'yarn' (Figure 2c) provided more than threefold gains in the ultimate tensile load (4.0 ± 0.4 fold, $p < 0.05$, Figure 2b) and toughness (5.0 ± 0.6 fold, $p < 0.05$, Figure 2c). The ultimate tensile strength (Figure 2b) and the Young's modulus increased by 30% and 20% respectively, as a result of twisting threads as yarns (Figure 2b,c).

The mechanical properties of the yarn were comparable to those of the native tendon.[14,15] Importantly, the load displacement profile of the twisted yarn mimicked the classical toe region of tendon/ligament tissue where the initial deformation is compliant and becomes stiffer with deformation. Pin-weaving of the ELAC yarn (Figure 1d) resulted in a highly porous ELAC bioscaffold (81 ± 5%) (Figure 1e) with a controlled and consistent scaffold morphology (Figure 1f). The wavy weaving pattern of ELAC yarn at the macroscale emulates the crimp in tendon. The load-displacement curve of a woven scaffold exhibited the initial compliant toe-region followed by a stiffer linear region with increasing displacement, a hallmark behavior of

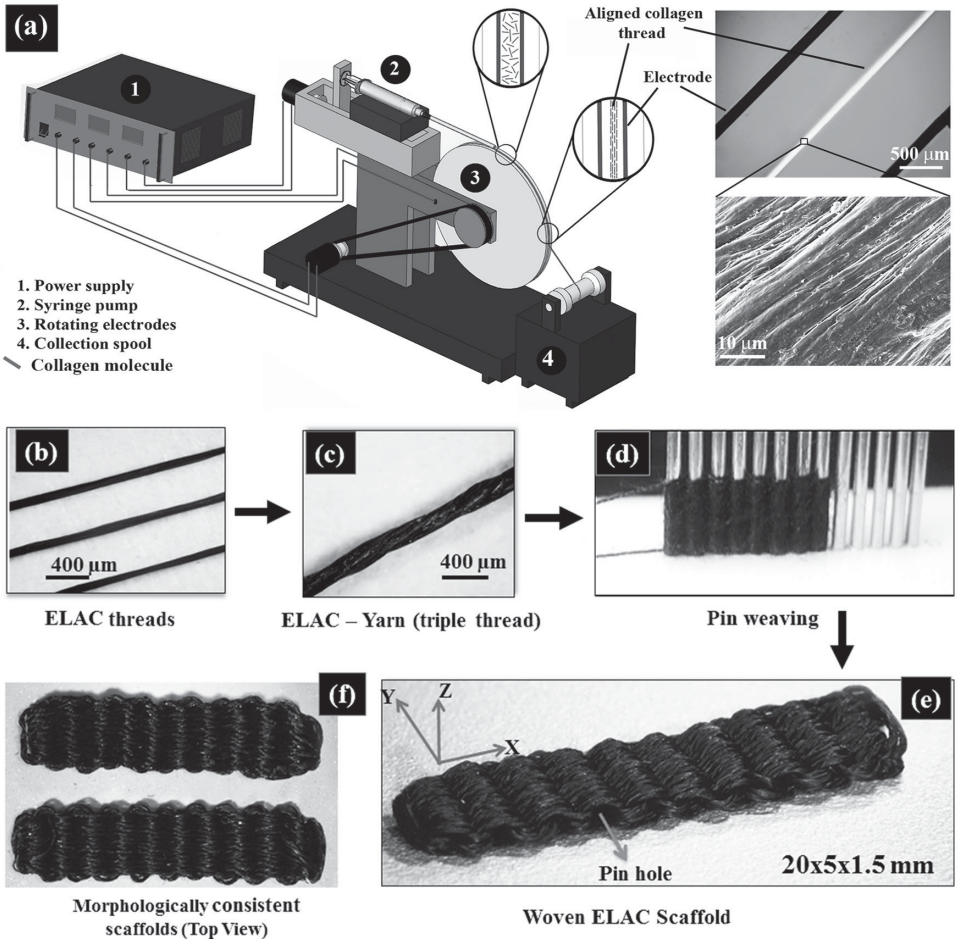

Figure 1. Schematic of the rotating electrode electrochemical alignment device (a). The main parts of the device are: power supply for providing voltage for the electrochemical cell, the syringe pump, rotating electrodes wheel and collection spool. Compensated polarized image in the top left inset demonstrates the collagen molecules to be aligned parallel to the longer axis of the thread as manifested by the blue color. Closely packed and aligned topography of the fiber surface is evident from the electron microscopy image. (b) Collagen fiber made by a rotating electrode electrochemical aligning device (REEAD), (c) yarn made by twisting three collagen threads, (d) pin-setup for weaving the collagen scaffold, (e) the resulting woven collagen scaffold, (f) and two scaffolds to demonstrate the consistency of fabrication.

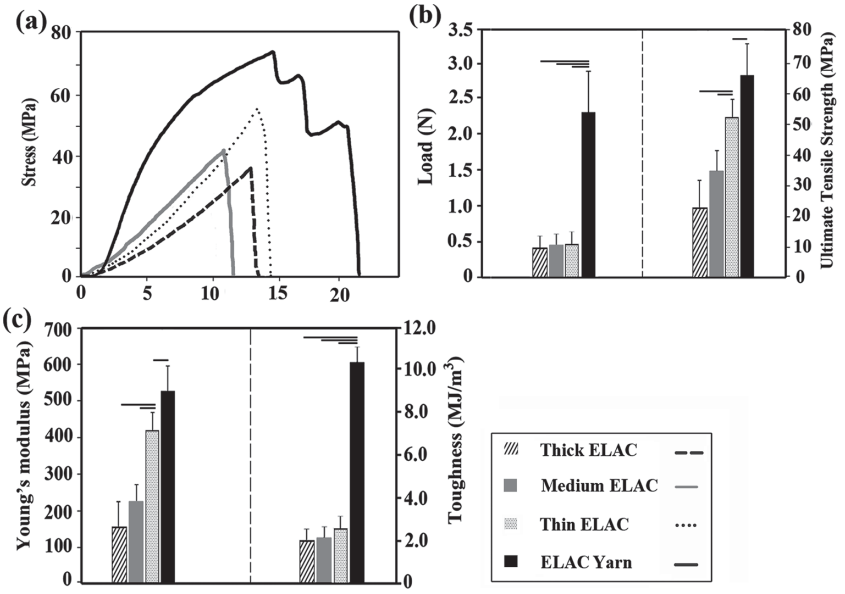

Figure 2. Mechanical assessment of ELAC threads with three different thicknesses and ELAC yarn. (a) Typical stress-strain curves of ELAC threads and ELAC yarn, (b) Failure load and strength of ELAC yarn is greater than individual ELAC threads, (c) toughness and Young's Modulus of ELAC yarn was greater than those of ELAC threads. The horizontal line indicates significant difference ($p < 0.05$).

tendon's deformation (**Figure 3**). The functional strength of the ELAC bioscaffold was about 60% of the strength of a comparably sized intact rabbit infraspinatus tendon. Moreover, the slopes of load-displacement curves for both tendon (28.5 ± 4.6 N/mm) and scaffold (23.8 ± 1.6 N/mm) were comparable in the linear regions of the curves, illustrating the proximity of scaffold's stiffness to that of the intact tendon. Together, these results demonstrate that the mechanics of 3D-woven scaffolds of electrochemically aligned collagen reproduced the functional mechanics of the native tendon in several key regards.

The woven scaffold provides favorable mechanics at 81% porosity. The porosity is important for populating the continuum of the scaffold uniformly with the cells at the time of cell-seeding. Histological sections at day 3 revealed that the mesenchymal

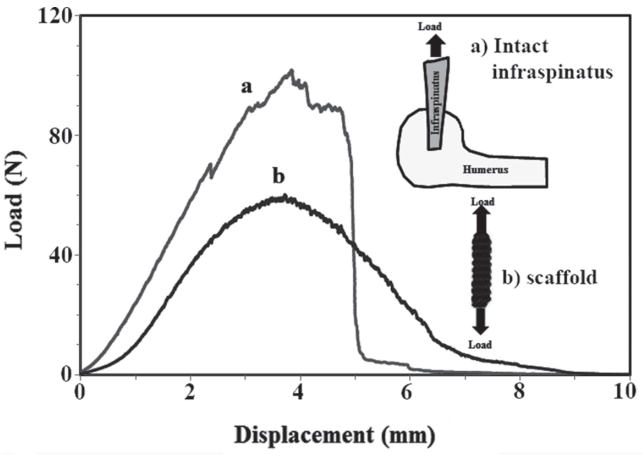

Figure 3. Tensile behavior of the scaffold (a) converges to that of similarly sized rabbit infraspinatus tendon (b).

stem cells were uniformly distributed within the scaffold (**Figure 4**a). The cells were mostly round at day 3 (Figure 4a); however, they assumed an elongated spindle shaped morphology close to the ELAC fibers on day 35 (Figure 4b,c). This observation indicates that the aligned topography of ELAC threads (Figure 1a) produced a cellular morphological phenotype similar to that of tenocytes.

Tendon-specific and tendon-related markers were up-regulated significantly on the ELAC threads compared to randomly oriented collagen fibers while bone-related markers were down-regulated. Type-I collagen was expressed at significantly greater ($p < 0.05$) levels on ELAC threads than randomly oriented collagen at all time-points, up to 3.4 ± 0.4 fold at day 14 (**Figure 5**a). Tenomodulin, a tendon specific marker, was about 10-fold higher on ELAC at days 14 and 21 when compared to randomly oriented collagen fibers (Figure 5b). Cartilage oligomeric matrix protein (COMP) was up-regulated by 6-fold at day 7 and 16-fold at day 14 on ELAC compared to randomly oriented collagen fibers (Figure 5c).

On the other hand, alkaline phosphatase (ALP) and Runt-related transcription factor 2 (RUNX2) expressions were 3-fold and 2-fold lower ($p < 0.05$) on ELAC thread at day 21 compared to day 1. Furthermore, osteocalcin expression level didn't change on ELAC threads with time and the expression of osteocalcin by cells seeded on ELAC threads was significantly lower ($p < 0.05$) than the expression by cells seeded on random gel. Together, these results indicate that the topographical alignment of ELAC (Figure 1a) stimulates the tenogenic differentiation of human MSCs.

Importantly, the gene-level expression of these tendon-markers was translated to the protein-level synthesis. Immunostaining of ELAC bioscaffolds at day 35 showed a fibrillar network within the pore space that is richly positive for type-I collagen (**Figure 6**a). Human MSCs synthesizing type-I collagen was also present on the surfaces of ELAC threads. Additionally, tendon markers tenomodulin and COMP were positive in the scaffold network (Figure 6b,c).

Transmission electron microscopy (TEM) revealed that the collagen associated with the ELAC threads was morphologically distinguishable from cell produced collagen. Specifically, collagen in ELAC was composed of thin microfibrils with diameters of 8.6 ± 1.2 nm (**Figure 7**a). The collagen matrix synthesized on ELAC threads by the cells was composed of thick fibers with diameters of 74.3 ± 8.8 nm which exhibited D-banding (Figure 7b), implying a matrix deposition consistent with immature tendon.

3. Discussion

We have demonstrated that a 3D scaffold that is woven from anisotropically oriented collagen threads has a significant

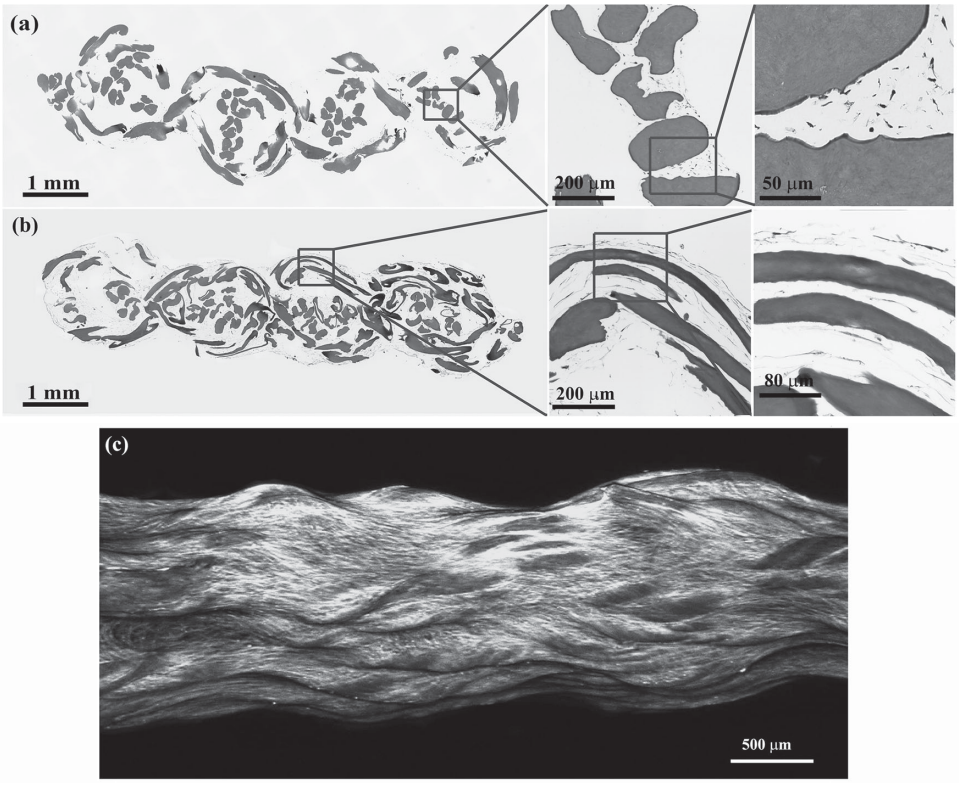

Figure 4. Histological sections of the ELAC bioscaffold stained with H&E at day 3 (a) and at day 35 (b). (a) High magnification image shows uniform distribution and penetration of cells within the ELAC bioscaffold at day 3. Cells have round morphology at this point in time. (b) Spindle shaped elongated cell morphology was observed around the ELAC threads by day 35. (c) A macrograph of cell-seeded scaffold where the cellular F-actin cytoskeleton is labeled. Cells have profusely covered the entire scaffold with elongated morphology.

tenogenic influence on MSCs by presenting evidence on the expression and production of tendon specific and tendon related markers. Up-regulation of the gene expression for functional markers was evident as early as day 7. These markers were consequently deposited by cells in the *de novo* matrix and COMP was present at the cell level while the expressions of bone-related markers were down-regulated.

To date, all reported biological textiles are woven from synthetic polymers.[10,16] To the best of our knowledge, this is the first time a scaffold of this mechanical robustness is woven purely from an ECM derived molecule. An ECM-derived scaffold presents the sites for cell attachment and also the amino acid sequences which are amenable to site specific digestion by matrix metalloproteinases synthesized by cells. Type-I collagen is non-immunogenic and less prone to foreign body reaction that is encountered with synthetic polymers. The weaving pattern employed in this study provided a mechanically competent structure at a volumetric porosity of 81%. This structure enabled the loading of cells across the entire scaffold volume expeditiously as evidenced histologically at day 3. This is an improvement over bulk scaffolds where the cellularization is bound to occur by surface to core degradation.

The reported tenogenesis is highly significant because there are no well accepted growth factor formulations for reliable attainment of tenoinduction, unlike osteogenic[17] and chondrogenic[18] induction of MSCs by cytokines. Marrow and adipose derived stromal cells showed tenomodulin expression[5,6,8,19,20] and in one case tenomodulin synthesis was reported[19] in the presence of growth factors. Various studies have shown topographical tenoinduction only at the expression level.[7,21] To the best of our knowledge, there are no studies which showed collagen, tenomodulin and COMP synthesis by differentiated MSCs only by topographical cues and in the absence of growth factors as we have demonstrated in this study.

Differentiation of MSCs to different lineages solely under the physical cue of substrate stiffness has been reported earlier.[22] The physical cue that is playing a role in the reported tenogenesis of MSCs is likely the anisotropic alignment of the ELAC collagen (Figure 1a). Mature tendon cells have elongated morphology and the aligned topography is also encountered during the embryogenesis of the tendon.[23] The cells within the 3D woven scaffold niche became elongated as dictated by the alignment of the collagen substrate (Figure 4b,c). Previous studies have reported the expression of tenogenic markers in a set of aligned biomaterials;[5,7,15] however, this outcome has not been attained in a 3D environment and confirmed at the matrix production level as demonstrated in this study. Therefore, aligned topography appears to be a necessary element for tenogenesis. The cell signaling mechanisms by which the elongated cell morphology provides a positive feedback to tenogenic differentiation remains to be elucidated.

Type I collagen was deposited in the scaffold in the pore regions as well as on the threads themselves. The structures of collagen fibers deposited in these regions differed substantially

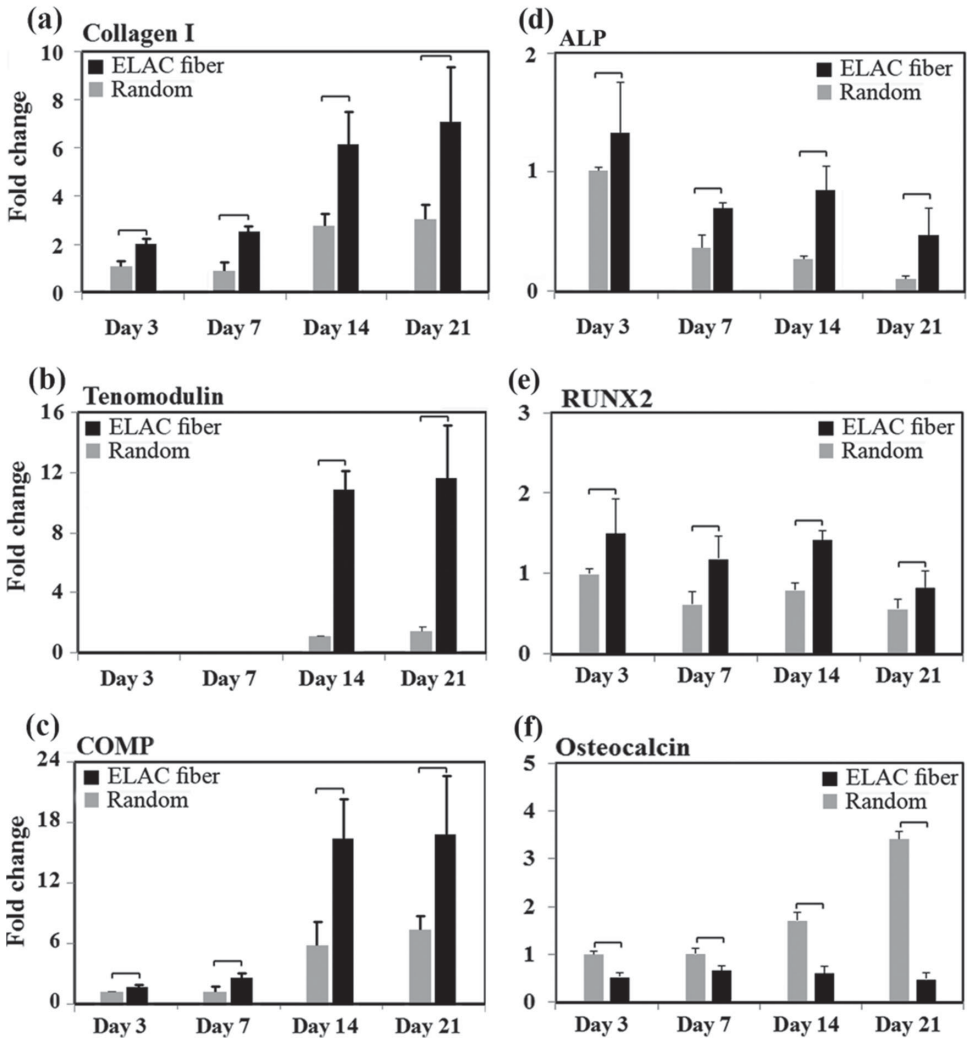

Figure 5. Topographical cues from the scaffold guide cells toward expression of the tendon specific/related proteins. RT-PCR results show significant up-regulation of Collagen I (a), tenomodulin (b), and COMP (c) on ELAC threads compared to random collagen samples at every time point. However, the expression of bone-related markers ALP (d) and RUNX2 (e) decreased over time. Osteocalcin expression was greater on random gel in comparison to ELAC threads. The expression of osteocalcin increased with time on random gels and did not change appreciably on ELAC threads. All bar graphs are normalized by expression at day 3 random group. The horizontal lines indicate significant differences ($p < 0.05$) between expressions of the markers on random collagen samples vs. ELAC threads.

in terms of their morphology. Electron microscopy indicated that the collagen fibers deposited directly on ELAC threads were densely packed and thick collagen fibers with d-banding pattern (Figure 7c). On the other hand, the collagen network deposited in the pore space was in the form of a loose network of thin collagen fibers (Figure 6a) which lacked d-band periodicity. This difference in morphology implies that cells closer to ELAC threads' are more heavily induced towards tenogenesis than cells which are further away from the threads. Therefore, a scaffold woven by smaller diameter threads would present a greater surface to volume ratio and increase the positive effects of the alignment induced differentiation cue. Other modification to enhance de novo collagen deposition would be mechanostimulation and assessing aligned threads with different substrate stiffness values. Kuo et al.[23] reported that the lateral modulus of tendon laid down during embryogenesis to be 10–100 kPa. The lateral moduli of fully crosslinked aligned collagen are 31 ± 9 MPa and 250 ± 82 MPa, respectively. These values are greater than those encountered in actively forming tissues. Therefore, it is possible that an aligned substrate with decreased levels of crosslinking to attain a lower modulus than the present threads may synergize with the alignment cue and increase the tenogenesis further.

The load-displacement curve of the woven collagen scaffold showed a characteristic behavior similar to native tendon where the stiffness increased gradually in a nonlinear fashion. The basis of this deformation pattern in the native tendon is in the observed crimp structure at the microstructural level of tendon, the so-called crimp. The weaving pattern of the present scaffold emulated the crimp-like pattern of tendon, albeit at the millimeter scale, resulting in a structural mechanical performance that is comparable to that of the native tendon.

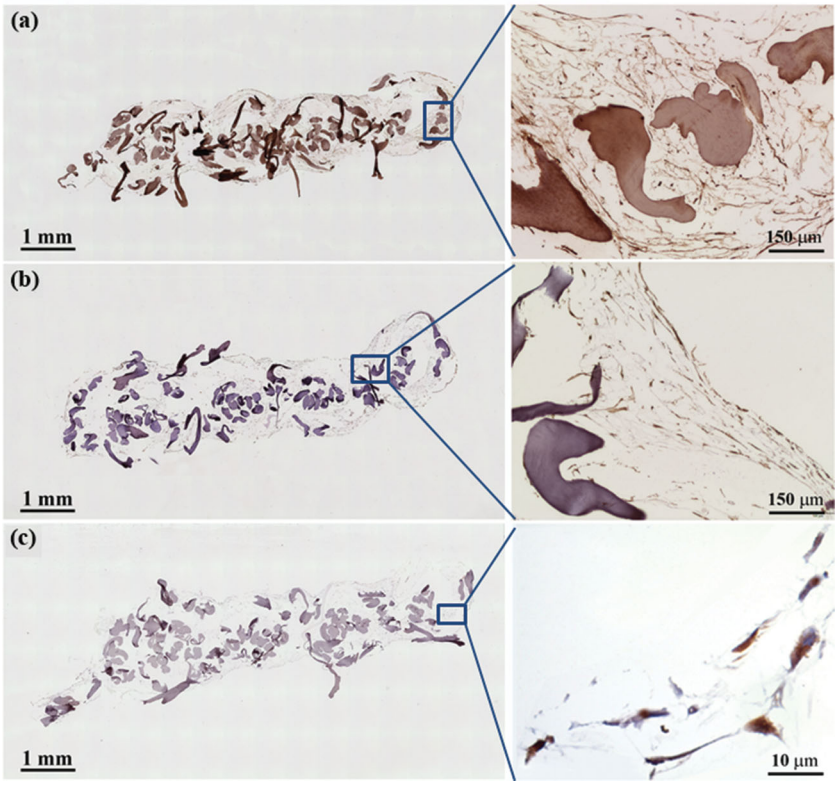

Figure 6. Immunohistochemistry of ELAC bioscaffolds for tendon-specific and tendon-related markers (Day 35). Type I collagen deposition was observed within the pores of the ELAC bioscaffold (a). Sections were positive for the tendon specific marker tenomodulin (b), and the tendon-related marker COMP (c).

Mechanical robustness is an essential characteristic for scaffolds to be used in musculoskeletal repair not only because such tissues are load bearing, but also resilience is needed for their surgical implantation. From a mechanotransduction perspective, the convergence of scaffold mechanical properties to that of tendons may aid in differentiation by providing a physiologically relevant milieu in terms of the magnitude of mechanical strain.

Prior studies from our group indicated that the electrochemically aligned threads which are crosslinked under similar conditions with those employed in this study was biocompatible and the degradation took place in a time frame between 4 to 8 months in vivo.[24] Based on the reported improvements in the mechanical robustness, the ease of cellularization and the tenogenic induction capacity of the woven scaffold model, an in vivo evaluation of this collagen biotextile is the essential next step to assess the vascularization and de novo tissue formation.

4. Experimental Section

Continuous Production of Electrochemically Aligned Collagen Threads: Acid soluble monomeric collagen solution (derived from bovine hide, Advanced Biomatrix, CA; 6 mg/mL) was diluted two-fold, pH adjusted between 8–10 using 1N NaOH and dialyzed against ultrapure water for 18 h. Electrochemically aligned collagen (ELAC) threads were fabricated by using a custom-made rotating electrode electrochemical alignment device (REEAD). The basic components of REEAD include electric motors, a syringe pump, a rotating electrode drum and a rotating collection spool (Figure 1a). Three different electric motors driven by a DC power supply were employed to drive: 1) the syringe pump, 2) the rotating electrode, and 3) the collection spool. The syringe pump houses a 10 mL syringe loaded with dialyzed collagen solution. The rotating electrode drum has a circumferential groove that is 2 mm in depth and 2 mm in width. Within the groove are two parallel electrodes wires (stainless steel) that are 1.6 mm apart. This configuration provides an 'infinite' length electrode due to the constant rotation. The syringe pump applies the dialyzed monomeric collagen solution at the top of the drum; the solution gets trapped in the groove and rotates with the drum. During rotation, the solution is subjected to the electric current and undergoes packing and alignment along the isoelectric point resulting in the formation of the ELAC thread by the time the drum completes one third of turn (~60 s). The thread is then released from the drum and spun onto a collection spool. The diameter of threads can be regulated by changing the rotational speed of the drum, such that, when the drum is rotated at faster speeds less collagen is applied between the electrodes. As such, ELAC threads with three different diameters were fabricated: thin (0.10 ± 0.03 mm), medium (0.13 ± .04 mm) and thick (0.15 ± 0.05 mm). The resulting ELAC threads are incubated in phosphate buffered saline (PBS) for six hours at 37 °C to induce fibril formation and treated with 2-propanol solution for 12 hours. Finally, the ELAC threads are crosslinked with 0.625% genipin (Wako Chemical, Japan) in 90% v/v ethanol solution at 37 °C for 3 days.[13]

Assessment of Mechanical Properties of ELAC Fibers and ELAC Yarn: Three individual crosslinked ELAC threads were twisted together to make a yarn. The mechanical properties of individual threads and yarns (n = 10/group) were measured using an ARES rheometer (TA instruments, New Castle, DA) as described previously.[13] Briefly, 2 cm long samples were cut using a scalpel blade and the samples were hydrated in 1× PBS for 1 h prior to testing. ELAC samples were fixed directly onto the aluminum fixtures of the rheometer at a gauge length of 10 mm and subjected to monotonic tensile loading until failure at a strain rate of 10 mm/min. Care was taken to ensure that the ELAC samples are tested in the wet state by briefly rehydrating the sample using a wet Q-tip prior to testing. The fractured samples were used for average cross-sectional area measurement using a multiphoton confocal microscope (Leica TCS SP2) by measuring the wet area at three different locations along the length of the sample. Quantification of ELAC cross sectional area was done using Image J (ImageJ 1.47v, U.S. National Institute of Health, Bethesda, MD). The load-displacement data generated was used to compute the ultimate stress and ultimate strain of the samples. Young's modulus was determined by calculating the slope of the linear region of the stress-strain curve.

Assessment of Tenogenic Differentiation on ELAC: Genipin crosslinked ELAC fibers and random collagen fibers (cut out from a genipin crosslinked collagen gel) were cut into 2 cm long pieces, sterilized with 70% ethanol and placed in an ultralow attachment 6-well plate (Corning). The culture medium composed of alpha MEM (Invitrogen) supplemented with 10% MSC-FBS (Invitrogen) and 1% penicillin/streptomycin. Human MSCs (P5; Lonza) were seeded at a density of 15 000 cells/cm^2 based on the area of the culture well and allowed to attach for 4 h. Unattached cells were removed by replacing the culture medium and the adherent cells were cultured for 21 days. At periodic intervals (days 3, 7, 14 and 21), the total RNA was extracted by lysing the cells using TRIzol Reagent (Life technologies, NY, USA) and following the manufacturer's instructions. Next, 1 µg of RNA was reverse-transcribed

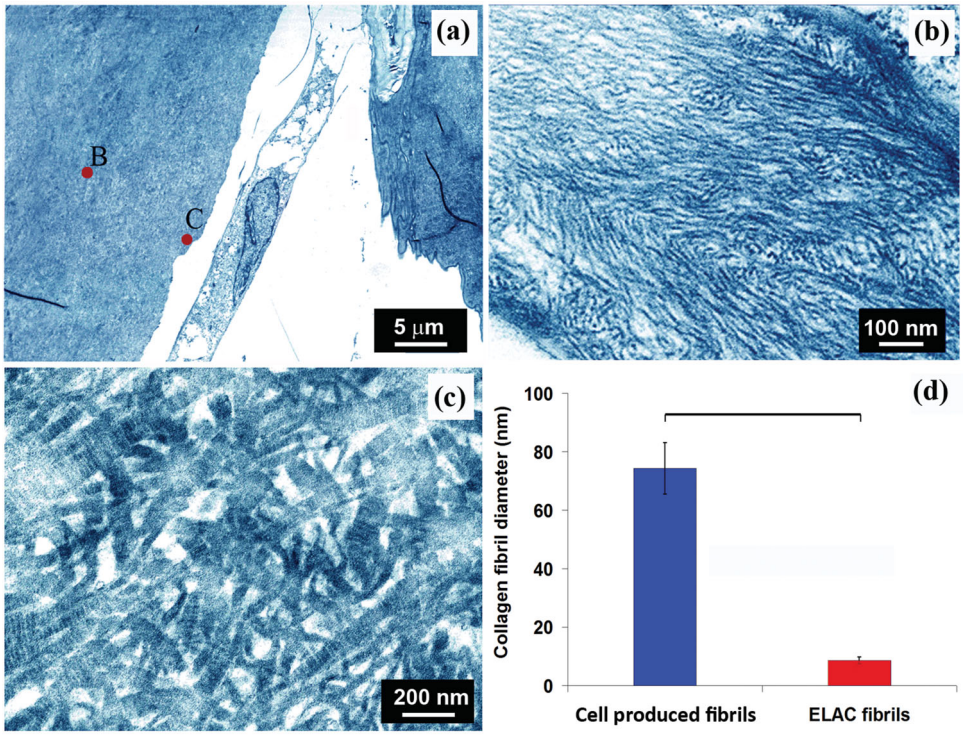

Figure 7. (a) Transmission electron microscopy images of collagen ultrastructure in woven scaffold seeded with cells at day 35. The core region of ELAC thread is highlighted as 'B' and the surface of the thread is highlighted with 'C' close to which an elongated cell is present. (b) Morphology of collagen fibrils of ELAC thread, and c) collagen fibers on thread surfaces synthesized by cells at day 35 displayed d-banding pattern which was absent in the fibrils of ELAC threads (b). (d) Average diameters of collagen fibers in ELAC thread and cell produced collagen. The horizontal line indicates significant difference ($p < 0.05$).

to cDNA using High-Capacity cDNA Reverse Transcription Kit (Applied Biosystems, CA, and USA). Taqman gene expression assays for type-I collagen, tenomodulin, COMP, ALP, RUNX2, and osteocalcin were used with the cDNA to evaluate the expression of genes using real-time PCR (Applied Biosystems 7500 Real-Time PCR System). The relative fold change in target gene expression was quantified using the 2^(-deltadeltaCt) method (TaqMan Gene Expression Assays Protocol, Applied Biosystem, life technologies) by normalizing the target gene expression to RPLP-0 and relative to the expression on the random collagen control at day 3. PCR experiments were run in triplicate at separate times.

Fabrication of Electrochemically Aligned Collagen Bioscaffolds: ELAC yarn was used to manually fabricate bioscaffolds using a pin-weaving method. Briefly, an array of 1 mm diameter pins was secured equidistantly (0.5 mm) from each other onto a solid substrate and an ELAC yarn was woven in a zig-zag pattern around the pins up to the desired width of the bioscaffold. The number of pins and size of pins determine the length and thickness of the bioscaffold, respectively. Once the weaving is complete, 10% PLGA solution was applied onto the bioscaffold and the bioscaffold was gently slid out of the pins, with the former location of the pins left out as holes. An ELAC yarn was then sutured through these holes to hold the woven threads together and result in the final bioscaffold (Figure 1b and e). The resultant bioscaffold was briefly submerged in chloroform to remove the PLGA coating. A total of seven scaffolds were fabricated for assessing the mechanical properties ($n = 3$) and cell response ($n = 4$).

Assessment of Mechanical Properties of Electrochemically Aligned Collagen Bioscaffolds: Woven scaffolds were tested under monotonic tension until failure under displacement-control (Test Resource 800LE3–2, Test Resources Inc., MN, USA). All the scaffolds were hydrated in water for 60 min before testing. Scaffolds were gripped by a tensile fixture at a gauge length of 10 mm. A 250 N load cell was used to measure the load. Three woven scaffolds were tested at a strain rate 10 mm/min.[13] Humerus-infraspinatus-muscle units were dissected from rabbits (Fresh frozen carcasses procured from Pel-Frez, New Zealand White, 1 year old, female). Samples were gripped at the muscle by custom grips at a minimum of 15 mm distance to the tendon portion by freezing the muscle with dry ice and the humeral head was potted in plastic cement (Millennium Pour Denture Acrylic, Cherry Hill, NJ). The samples were loaded monotonically at a rate of 10 mm/min until failure (Test Resource 800LE3–2, Test Resources Inc., MN, USA).

Cell Seeding in ELAC Bioscaffolds: ELAC bioscaffolds fabricated by using the pin-weaving method were sterilized in 70% ethanol and placed in an ultralow attachment 24-well plate (1 scaffold/well). The scaffold dimensions were 10 mm × 5 mm × 1.5 mm. The culture medium composed of alpha MEM (Invitrogen) supplemented with 10% MSC-FBS (Invitrogen), 1% penicillin/streptomycin and 50 μg/mL ascorbic acid. The ELAC bioscaffolds ($n = 4$) were air dried prior to cell seeding and then seeded with passage-5 human mesenchymal stem cells (Lonza) using the following method: A highly concentrated cell suspension (4 million cells/mL) was added dropwise onto the scaffold using a fine pipette in 25 μL increments such that a total of 500 000 cells were seeded onto each scaffold. The cells were allowed to attach by incubating the scaffolds at 37 °C for 3 h. To ensure that the scaffold remains hydrated during this time, 10 μL droplets of culture medium was added every hour. After 3 h, 1 mL of culture medium was added to each well and the scaffolds were cultured for 35 days. At days 3 and 35 bioscaffolds were fixed in 10% neutral buffered formalin and subjected to histological processing for analyses.

Histology and Immunohistochemistry for Cell Distribution and De Novo Matrix Production: Formalin-fixed ELAC bioscaffolds were subjected to paraffin embedded histology and immunohistochemistry to assess cell penetration within the scaffold and *de novo* matrix synthesis. For histological assessment, 5 μm thickness sections were stained with

using hematoxylin and eosin to assess cell viability, penetration and distribution within the scaffold. Immunohistochemistry was performed for matrix typification (Col-I) and assessment of the protein-level expression of tendon-specific markers (tenomodulin and COMP). The histological sections were baked at 60 °C for 75 min, deparaffinized with xylene, rehydrated with a graded series of ethanol and rinsed with water. For antigen retrieval, the sections were hydrated for 30 s, incubated in citrate buffer (Vector Laboratories, Burlingame, CA) for 5 minutes in a steamer at 98 °C and allowed to cool on a bench top for 20 min. The endogenous peroxidase activity was blocked by incubating the sections in peroxidazed-1 (Biocare Medical, Concord, CA) for 8 min. Following this, biotin and avidin activity was blocked by incubating the sections in two separate solutions of an Avidin Biotin kit (Biocare Medical) for 15 min each. The endogenous IgG and background protein activity was blocked by incubating the sections in a background sniper solution (Biocare Medical) for 20 min. The sections were then rinsed with TBST (Tris Buffered Saline + 0.05% Tween 20) prior to staining with the primary antibody. Anti-human primary antibodies for type-I collagen (rabbit polyclonal, Rockland Immunohistochemicals Inc., Gilbertsville, PA), tenomodulin (goat polyclonal, SantaCruz Biotechnology, Dallas, TX) and COMP (rat monoclonal, SantaCruz Biotechnology, Dallas, TX) were diluted in a protein block serum-free antibody diluent (Dako, Carpinteria, CA) with ratios of 1:200 for collagen antibody, 1:50 for tenomodulin and COMP antibodies. The sections were incubated with the primary antibody for 1 h at room temperature and then rinsed with the TBST solution. The collagen stained slides were incubated with MACH4-HRP Polymer (BioCare Medical) for 30 min and then rinsed with TBST solution. The tenomodulin stained sections were incubated with the biotinylated mouse-anti goat IgG HRP polymer (Biocare Medical) for 30 min, rinsed with TBST and then incubated with Betazoid DAB (Biocare Medical) in the dark for 5 min. The COMP stained sections were incubated with a Rat Probe (Biocare Medical) for 20 min, rinsed with TBST and then incubated with Rat Polymer HRP for 20 min. Following this, all the sections were counterstained with CAT hematoxylin (Biocare Medical), rinsed with water and cover slipped. Sections treated similarly but without the primary antibody served as the negative control.

Collagen Fiber Morphology by Transmission Electron Microscopy: Blank collagen threads and cell-seeded scaffolds at day 35 were fixed by immersion in the quarter strength Karnovsky fixative solution for 2 hours at room temperature. After washing, the specimen was post-fixed for 2 h in an unbuffered 1:1 mixture of 2% osmium tetroxide and 3% potassium ferrocyanide. After rinsing with distilled water, specimens were soaked overnight in an acidified solution of 0.25% uranyl acetate, rinsed in distilled water, dehydrated in ascending concentrations of ethanol, passed through propylene oxide, and embedded in a Poly/Bed 812 embedding media (Polysciences, Warrington, PA). Thin sections (70 nm) were cut on an ultramicrotome (RMC MT6000-XL), mounted on Gilder square 300 mesh nickel grids (Electron Microscopy Sciences, PA) and sequentially stained with acidified methanolic uranyl acetate and stable lead staining solution. Samples were coated on a Denton DV-401 carbon coater (Denton Vacuum LLC, NJ), and examined with a JEOL 1200EX electron microscope (Tokyo, Japan).

Statistical Analysis: Differences between groups (mechanical properties of the ELAC threads and yarn, PCR results at every time points for random collagen and ELAC thread and also collagen fibers diameters in ELAC threads and cell produced collagen fibers) was assessed using a 2-sample student t-test. For all tests, the level of significance was set at $p \leq 0.05$.

Acknowledgements

This study was funded in part by grants from the National Science Foundation (Grant Number DMR-1306665), National Institute of Health (Grant Number R01 AR063701), and the AO Foundation. Any opinions, findings, and conclusions or recommendations expressed in this material are those of the author(s) and do not necessarily reflect the views of the National Science Foundation. The authors would like to thank Adam Kresak for his help with immunohistochemistry, Amad Awadallah for help in histology staining and Yunus Alapan for his assistance in imaging of the immunohistology slides.

Received: March 13, 2014
Revised: May 7, 2014
Published online: July 17, 2014

[1] a) A. R. Baker, J. A. McCarron, C. D. Tan, J. P. Iannotti, K. A. Derwin, *Clin. Orthop. Relat. Res.* **2012**, *470*, 2513; b) E. T. Ricchetti, A. Aurora, J. P. Iannotti, K. A. Derwin, *J. Bone. Joint Surg. Am.* **2012**, *21*, 251; c) L. B. Wall, J. D. Keener, R. H. Brophy, *J. Bone. Joint Surg. Am.* **2009**, *18*, 933.

[2] a) P. B. van Wachem, T. Beugeling, J. Feijen, A. Bantjes, J. P. Detmers, W. G. van Aken, *Biomaterials* **1985**, *6*, 403; b) Y. Wan, W. Chen, J. Yang, J. Bei, S. Wang, *Biomaterials* **2003**, *24*, 2195.

[3] a) H. Xu, H. Wan, M. Sandor, S. Qi, F. Ervin, J. R. Harper, R. P. Silverman, D. J. McQuillan, *Tissue Eng. Part A* **2008**, *14*, 2009; b) A. G. Mikos, L. V. McIntire, J. M. Anderson, J. E. Babensee, *Adv. Drug. Deliv. Rev.* **1998**, *33*, 111.

[4] K. A. Derwin, M. J. Codsi, R. A. Milks, A. R. Baker, J. A. McCarron, J. P. Iannotti, *J. Bone. Joint Surg. Am.* **2009**, *91*, 1159.

[5] S. L. Tan, R. E. Ahmad, T. S. Ahmad, A. M. Merican, A. A. Abbas, W. M. Ng, T. Kamarul, *Cells, Tissues, Organs* **2012**, *196*, 325.

[6] a) W. Chai, M. Ni, Y. F. Rui, K. Y. Zhang, Q. Zhang, L. L. Xu, K. M. Chan, G. Li, Y. Wang, *Chin. Med. J. (Engl)* **2013**, *126*, 1509; b) M. Ni, Y. Rui, Q. Chen, Y. Wang, G. Li, *Chin. J. Reparative Reconstructive Surg.* **2011**, *25*, 1103; c) S. Violini, P. Ramelli, L. F. Pisani, C. Gorni, P. Mariani, *BMC Cell Biol.* **2009**, *10*, 29.

[7] V. Kishore, W. Bullock, X. Sun, W. S. Van Dyke, O. Akkus, *Biomaterials* **2012**, *33*, 2137.

[8] R. I. Sharma, J. G. Snedeker, *PloS One* **2012**, *7*, e31504.

[9] T. K. Teh, S. L. Toh, J. C. Goh, *Tissue Eng. Part A* **2013**, *19*, 1360.

[10] J. G. Barber, A. M. Handorf, T. J. Allee, W. J. Li, *Tissue Eng. Part A* **2013**, *19*, 1265.

[11] H. K. Kleinman, R. J. Klebe, G. R. Martin, *J. Cell Biol.* **1981**, *88*, 473.

[12] X. Cheng, U. A. Gurkan, C. J. Dehen, M. P. Tate, H. W. Hillhouse, G. J. Simpson, O. Akkus, *Biomaterials* **2008**, *29*, 3278.

[13] J. Alfredo Uquillas, V. Kishore, O. Akkus, *J. Mech. Behav. Biomed. Mater.* **2012**, *15*, 176.

[14] a) E. Itoi, L. J. Berglund, J. J. Grabowski, F. M. Schultz, E. S. Growney, B. F. Morrey, K. N. An, *J. Orthop. Res.* **1995**, *13*, 578; b) T. A. Wren, S. A. Yerby, G. S. Beaupre, D. R. Carter, *Clin. Biomech.* **2001**, *16*, 245.

[15] S. P. Lake, K. S. Miller, D. M. Elliott, L. J. Soslowsky, *J. Biomech.* **2010**, *43*, 727.

[16] a) F. T. Moutos, L. E. Freed, F. Guilak, *Nature Mater.* **2007**, *6*, 162; b) S. Sahoo, J. G. Cho-Hong, T. Siew-Lok, *Biomed. Mater.* **2007**, *2*, 169.

[17] a) M. D. Schofer, P. P. Roessler, J. Schaefer, C. Theisen, S. Schlimme, J. T. Heverhagen, M. Voelker, R. Dersch, S. Agarwal, S. Fuchs-Winkelmann, J. R. Paletta, *PloS One* **2011**, *6*, e25462; b) A. Martins, A. R. Duarte, S. Faria, A. P. Marques, R. L. Reis, N. M. Neves, *Biomaterials* **2010**, *31*, 5875.

[18] B. O. Diekman, N. Christoforou, V. P. Willard, H. Sun, J. Sanchez-Adams, K. W. Leong, F. Guilak, *Proc. Natl. Acad. Sci. USA* **2012**, *109*, 19172.

[19] J. Y. Lee, Z. Zhou, P. J. Taub, M. Ramcharan, Y. Li, T. Akinbiyi, E. R. Maharam, D. J. Leong, D. M. Laudier, T. Ruike, P. J. Torina, M. Zaidi, R. J. Majeska, M. B. Schaffler, E. L. Flatow, H. B. Sun, *PloS One* **2011**, *6*, e17531.

[20] a) A. Park, M. V. Hogan, G. S. Kesturu, R. James, G. Balian, A. B. Chhabra, *Tissue Eng. Part A* **2010**, *16*, 2941; b) R. James, S. G. Kumbar, C. T. Laurencin, G. Balian, A. B. Chhabra, *Biomed. Mater.* **2011**, *6*, 025011.
[21] M. S. Peach, R. James, U. S. Toti, M. Deng, N. L. Morozowich, H. R. Allcock, C. T. Laurencin, S. G. Kumbar, *Biomed. Mater.* **2012**, *7*, 045016.
[22] D. E. Discher, P. Janmey, Y. L. Wang, *Science* **2005**, *310*, 1139.
[23] J. E. Marturano, J. D. Arena, Z. A. Schiller, I. Georgakoudi, C. K. Kuo, *Proc. Natl. Acad. Sci. USA* **2013**, *110*, 6370.
[24] V. Kishore, J. A. Uquillas, A. Dubikovsky, M. A. Alshehabat, P. W. Snyder, G. J. Breur, O. Akkus, *J. Biomed. Mater. Res. B Appl. Biomater.* **2011**, *100B*, 400.